Control and Management of Railway System Connected to Microgrid Stations

P. Bhaskar Prasad[1], D.Veera Ganesh Kumar [2],M.Sindhu [3],P.Rajasri [4],K.Nitheesh [5]

[1]Assistant professor, Department of Electrical and Electronics Engineering, Annamacharya Institute of Technology and Sciences (AITS), Rajampet

[2,3,4,5] Student of Electrical and Electronics Engineering, Annamacharya Institute of Technology and Sciences (AITS), Rajampet

Abstract:

This research suggests a techno-economic approach for power storage in trains by using SCs, with a habit of lowering energy consumption. The newly proposed train station design having PV and wind energy sources, energy storage system (ESS)by using batteries. SCs are introduced into the train and supplied breaking phases and stations via a pantograph positioned on the train at each stop. SCs are used because of their high power storing capacity and a more number of cycles, as well as their low specific energy and rapid charging time. An energy management technique is provided , voltage is managed the DC bus and current manages buck-boost converter. The size of the PI controller used for railway and station DC bus stabilization is specified. The entire model is run in MATLAB-Simulink. The train and station simulations demonstrate the viability of the proposed powertrain and control techniques.

INDEX TERMS:

Supercapacitors, Energy Storage Systems, Railway System Control, and Energy Management.

1.Introduction

A. Motivation

Energy use and pollution have largely increased during the past few decades . As more people commute between cities, public transit systems like buses, taxis, and trains have had to develop continuously. However, due to their potential to carry a huge number of passengers, railroad transportation systems are increasingly preferred over other traditional modes of transportation. People can now travel swiftly thanks to the development of rail technology. Therefore, the need to improve the performance energy regulation of railway systems is dictated by developing environmental challenges like climate change and CO_2 emissions change. Due to these factors, electrified rail traffic has taken the lead in shaping the construction of the present public transportation systems .

Creating clean energy from renewable sources has emerged as one of the hottest social development issues [7]. Although diverse renewable energy sources, including as photovoltaics (PV) and wind turbines, are integrated into the railway system. An energy storage system (ESS) is required to guarantee a constant power supply and to react to the charge power of trains as they move from station to train [8], [9]. Numerous ESS technologies are employed in the railway system as a positive way to increase load needs in order to manage the overload fluctuation in the railway power supply structure during the heights of commuter hours [6], [10]. The weight and volume of a vehicle were increased by the on-board storage, which promoted subsurface storage.

With a high power density, a long lifespan, and a wide temperature range, SC_s are an emerging energy storage technology that has proven to be the optimum storage option for a railway SC_ssystem's operational features [11] through [14]. Due to its high power density and significant potential for energy recovery, SC_s have a fast charging and discharging time when compared to other energy storage devices like batteries and flywheels [15]. In general, ESS with SC is considered like energy buffer accelerating mode of train and recycles the excess of power during the braking mode. realizing a good balance of charge and discharge [16]. SC_s are considered a best solution in systems which characterized with different fluctuations. SC_s are also used in interruptible power systems to stabilized the power and bus voltage. The energy storage in railway system presents a challenge for researches [17], [18].Energy management systems (EMS) are currently a major challenge in large-scale complex energy distribution networks such as railway structures. The majority of EMS railway structure research is focused on technologically improving the railway system. EMS at the system level with an integrated strategy into the railway structure is frequently overlooked [19], [20]..Many articles [21, 22] present the optimal control theory for railway vehicles. EMS is used to control and connect various devices in the railway system, including energy storage devices, sources, and trains.

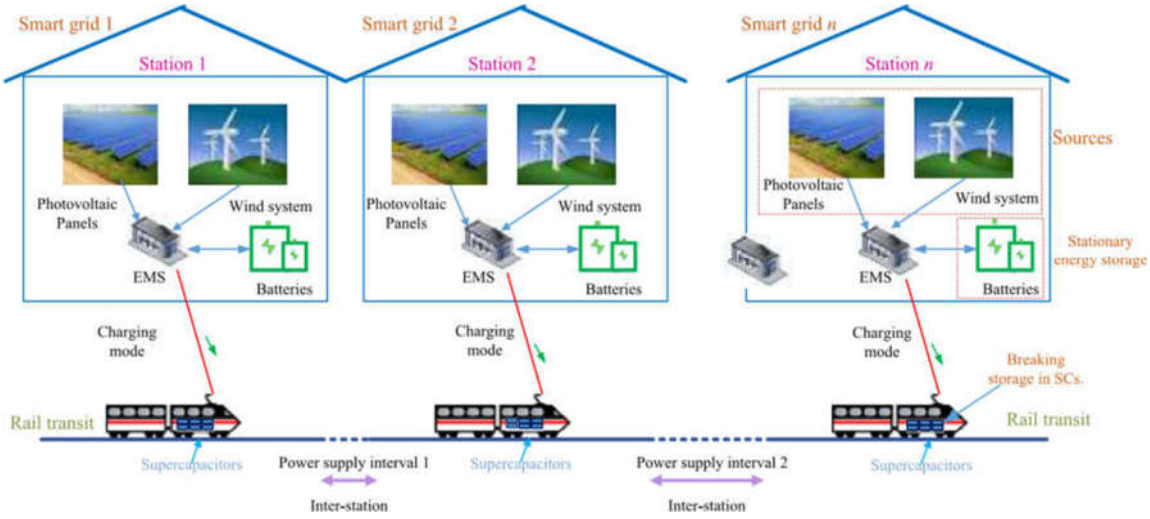

FIGURE 1. Train network traction characteristic

B. Literature

A fast inspection approach for high-speed railway infrastructure monitoring is presented by Jiang in one paper [23], while Feng proposes an electric railway smart microgrid system with the integration of diverse energy systems and power quality enhancement in another article [24]. Khayyam gives railway system energy management optimization demonstrated at offline and online case studies [19], Zhang presents the method using a prediction approach [24], He shown the energy harvesting approach for railway wagon monitoring sensor with high reliability and simple structure [25], Sun presents the hybrid method for life prediction of railway [26], Novak presents the hierarchical model predictive control for coordinated electric railway traction system energy management [27], Sensor gives the energy management of a smart railway station considering regenerative braking and stochastic behaviour of ESS and PV Generation [28].

C. Contributions

The proposed system is divided into two parts: the first deals with the stations, while the second is concerned with train control. The stations are made out of PV and wind farms, with batteries providing security for the energy storage. SC_s and engines make up the trains. Because of their tremendous power, SC_s are utilized. The following are the novel contributions made in this article:

• A train system that uses SC_s for energy storage that is fueled by stations and breaking phases.

• It is advised that a new EMS be used to manage the buck-boost converter's current and the DC bus voltage.

• The PI controller's size, which is utilized to stabilize the DC bus in trains and stations. a plan for a railroad station that makes use of solar and wind energy as well as batteries to store electricity.

The remaining paper is as follows: In Section II, a description of the system is shown. In Section II, the system modelling and management are developed. Section IV discussion of simulation and validation. The conclusion is reached in Section V.

2.System Description

A. Global System Description

The implementing of the rail transit and energy strategy is illustrated in Fig 1. The railway system is constructor of two systems. The first one is stationary system which represents the different stations. Each station is composed by a main energy sources which are PV panels and wind system. The energy provided from main sources is stored in batteries. Boost, buck-boost converters, and inverters all guarantee the conversion of energy. An inverter connects the wind system to the DC bus. PV panels are connected to the DC bus using a boost converter. In order to connect the batteries to the DC bus, a buck-boost converter is used. The components and construction of the various stations are the same. An EMS based on PI control ensures the control of the DC bus.

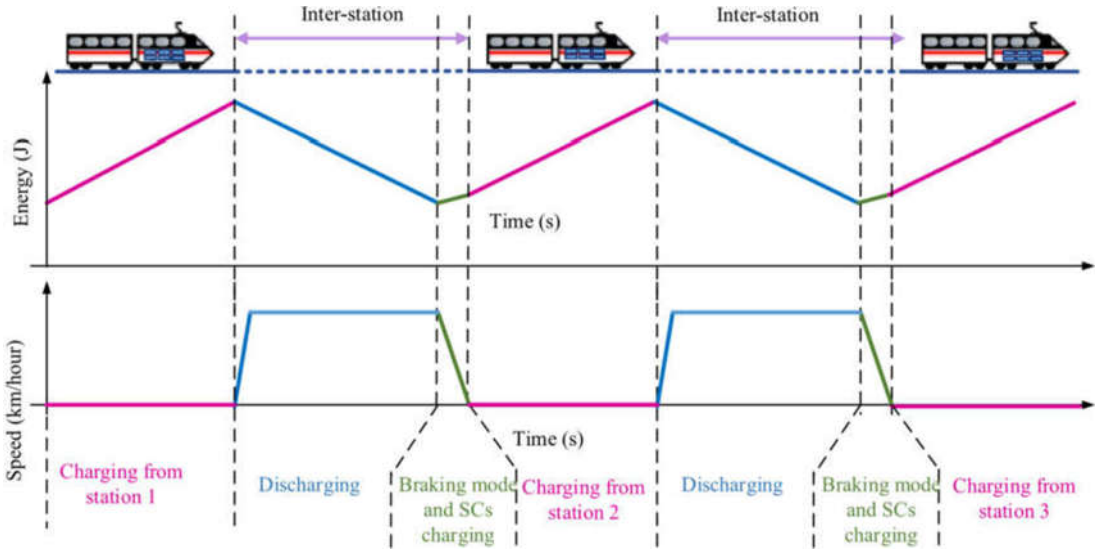

FIGURE 2. Power and speed change between train and stations.

The second is a movable system that simulates trains. Supercapacitors and motors make up each train. A buck-boost converter ensures that power is transferred from SC_s to the motors.

B. Distribution Of Energy Between Devices

The exchange of energy between different devices is given in Fig. 2. The railway system is divided in different stations. The distance between station is more than 10Km. Trains stop in each station between 5 and 15 minutes. During this trains stop, the motors train stop working and SC_s charge from batteries installed in the stationary station by a buck-boost converter. The charge of SC_s in the stations is insured by the pantograph connected the roof of the trains. The SC_s supply the energy required for the movement of the train between stations. The energy is transferred back to SC_s during the train's braking process. This energy, which is generated by various trains, will be locally stored and produced subsequently during the next phases of the train's acceleration.

Nevertheless, the train operates as a load when in tracking mode and as a power source when in braking mode. Trains and stations are linked and communicate with one another.

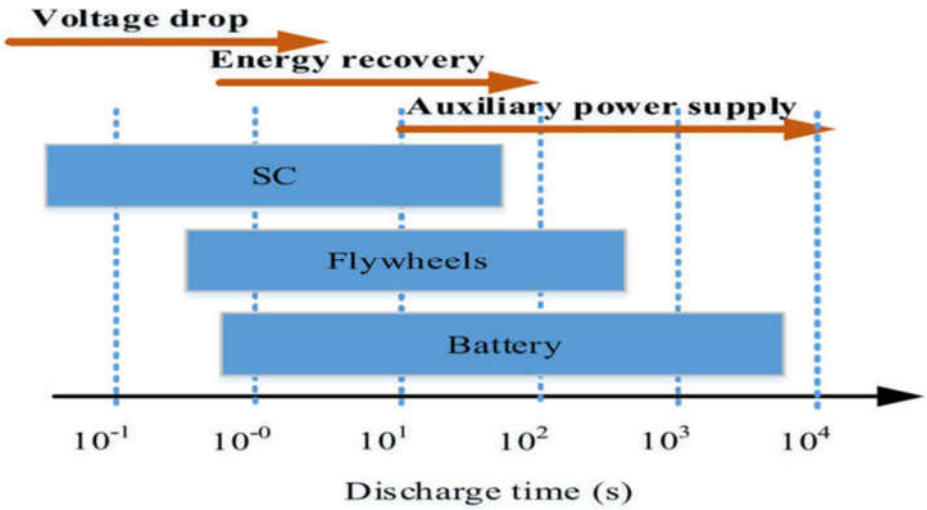

FIGURE 3. Classification of ESS technologies [22].

The form of electrical power exchange is resolved by the varied states of operation of rail train engines. The train is accelerating under the conditions when the engine is in alternator mode. In this instance, the traction mechanism converts the electric power circle's forward motion into kinetic energy. The train is in braking and deceleration mode during the traction engine, the power producing phase. The kinetic energy

produced by the train when braking is used by the auxiliary installations of the train, with the majority of them being sent back to the SC_s and used by the train in the same power supply phase. At this point, the electric energy circle is moving in the opposite direction.

By minimizing the power circle via the line and creating smoother voltage profiles, the installation of storage devices lowers energy line losses without the need to modify the building's infrastructure. However, the installation of SC_s on a vehicle requires a lot of room and adds extra weight, which can greatly impact the train's dynamic requirements.

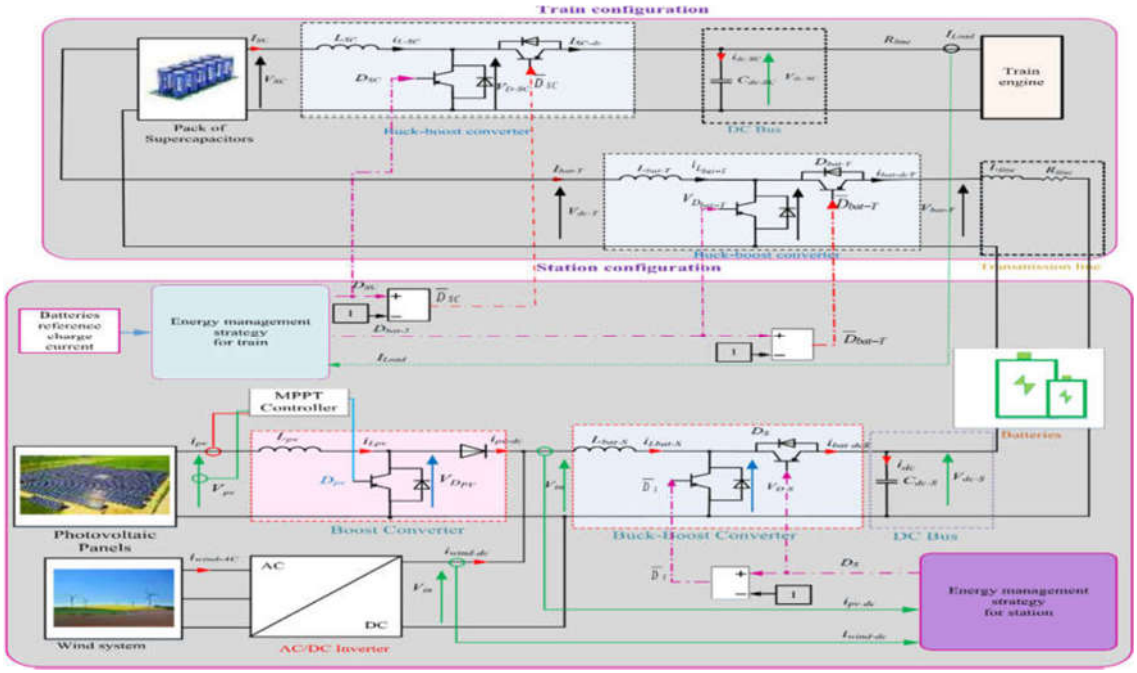

FIGURE 4. Configuration of the train model.

The train has 3.5 MW of power. The projected amount of energy delivered by SC_s is 210MJ, or 3.5MW for 60 seconds.

C. Choose Of Energy Storage Devices

The most suitable ESS technologies able to meet the railway system is presented in Fig. 3. Flywheels and supercapacitors are performed by high specific power and a large number of charge/discharge cycles. However, they present low specific energy [22]. In fact, they can be implemented in urban rail transit or metro stricture. Batteries represents a low discharge time. Supercapacitors present the fastest energy storage dispositive in terms of charging and discharging time. For this raison, the use of SC_s in the braking and acceleration phases gives good resultants and is the most suitable ESS devices for railway system.

III. SYSTEM MODELLING AND ENERGY MANAGEMENT

The control scheme for the DC bus is shown in Fig. 4. The Emergency Medical System is split into two sections; the first controls the stationary system, and the second is in the train.

The wind system generates AC power for stationary systems. A AC-DC converter is used to connect it to the DC bus. Using a Boost converter, the PV system is connected to the same bus. To stabilize the PV power and voltage, an MPPT maximum power point tracking system has been put into place. The DC bus voltage v_{dc} is stabilized, and the batteries are charged, using a Buck-Boost converter. A resistance and an inductance both contribute to a line transmission.

A Buck-Boost converter is used in the train system to link batteries to SC_s To pair SC's train engine and steady the voltage to 2KW, another Buck-Boost is used. To filter the power fluctuation from the converters, a capacitor is used in parallel with the engine and the buck-boost converter. The converters are controlled by the EMS. Table 1 provides the mathematical modelling of the PV and wind systems. Table 2 provides the mathematical modelling of SC_s and batteries. Two branches are modelled by the selected SC_s. CIMAT batteries are the type of batteries being used. Current flow can be reversed in the buck-Boost converter. This converter's modelling is shown in Fig. 5 [8].

Device	Mathematical model		Abbreviations
PV [22]	PV current I_{pv}	$I_{pv} = I_{ph} - I_d - I_r$ $I_s\left(\exp\left(\frac{q\left(V_{pv}+I_{pv}R_s\right)}{n_{s-pv}AkT_c}\right)-1\right)$ $\frac{I_{pv}R_s+V_{pv}}{R_p}$	I_{ph} : Photocurrent I_S : Cell dark saturation current $n_{s\text{-}pv}$: Number of PV cells T_C :Cell's working temperature T_n : Cell's reference temperature A : Ideal factor R_S : Series resistor R_p : Shunt resistor $I_{s,0}$: Cell's short-circuit current at a 25°C E_g : Energy of the band gap I_r : Solar irradiation I_{ph} : Light-generated current I_n : Solar irradiation at T_C temperature q: Electron charge k: Boltzmann's constant
	PV current I_{pv}	$I_{pv} = I_{ph} - I_s\left(\exp\left(\frac{q\left(V_{pv}+I_{pv}R_s\right)}{n_{s-pv}AkT_c}\right)-1\right)$ $-\frac{I_{pv}R_s+V_{pv}}{R_p}$	
	saturation current I_s	$I_s = I_{s,0}\left(\frac{T_n}{T}\right)^3 \exp\left[\frac{qE_g}{Ak}\left(\frac{1}{T_n}-\frac{1}{T}\right)\right]$	
	Photocurrent I_{ph}	$I_{ph} = \left(I_{ph,n} + K_I\Delta T\right)\frac{G}{G_n}$ $\Delta_T = T - T_n$	
Wind	power turbine P_m	$P_m = \frac{1}{2}C_p(\lambda,\beta)\rho\frac{A}{2}V_{wind}^3$	β : blade pitch angle C_p : performance coefficient λ : tip speed ratio of the rotor blade A : turbine swept area λi is a coefficient that is given by the following equation ρ : density of air.
	$C_p(\lambda;\beta)$	$C_p = \frac{1}{2}\left(\frac{116}{4}-0.4\beta-0.5\right)e^{-\left(\frac{21}{\lambda}\right)}$	
	λi coefficient	$\frac{1}{\lambda_i} = \frac{116}{\lambda+0.08\beta} - \frac{0.035}{\beta^3+1}$	
	wind turbine torque T_m	$T_m = \frac{1}{2}\rho\pi R^3\frac{C_p(\lambda)}{\lambda}v^2$ $= \frac{1}{2}\rho AC_p(\lambda)v^3\frac{1}{\omega_m}$	

TABLE 1. Mathematical modelling of PV and wind system

When the switch is closed during the active phase, the input voltage is provided by:

$vL - SC = Vsc = Lsc\frac{diL-SC}{dt}$ ..... (1) $\frac{diL-SC}{dt} = \frac{Vsc}{Lsc}$ .....(2)

where L_{SC} is the inductance,V_{SC} is the SC_S voltage, C_{dc-sc} is the SC_s buck-boost capacitor.

Since the switch is open during the Freewheeling phase, the inductor current cannot abruptly change. The following equations describe the input voltage

$vL - SC = Vsc - vdc = Lsc\frac{diL-SC}{dt}$ ..(3) $\frac{diL-SC}{dt} = \frac{Vs-vdcc}{Lsc}$ .....(4)

Device	Mathematical model		Abbreviations
SC [23]	SC voltage	$U_{SC} = N_{S-SC}v_{SC} = N_{S-SC}v_1 + R_1\frac{I_{SC}}{N_{P-SC}}$	C_0 : capacity (in F) C_v : constant parameter
	SC capacity	$C_1 = C_0 + C_v.v_1.$	
	v_2 voltage	$v_2 = \frac{1}{C_2}\int i_2 dt = \frac{1}{C_2}\int\frac{1}{R_2}(v_1 - v_2)dt.$	Q_1 : charge R_1C_1 presents the immediate behavior of SCs during fast charge/discharge R_2C_2 presents the internal energy distribution at the final of charge/ discharge
	current i_1	$i_1 = C_1.\frac{dv_1}{dt} = \frac{dQ_1}{dt} = \left(C_0 + C_v.v_1\right)\frac{dv_1}{dt}$	
	charge Q_1	$Q_1 = C_0.v_1 + \frac{1}{2}C_v.v_1^2$	
Battery [7]	Battery voltage	$V_{bat} = n_b.E_b + n_b.R_i.I_{bat}$	R_i: internal resistance of battery V_{bat} : battery voltage I_{bat} : battery current n_b : cells in series E_b: electromotive force as a function of the battery state of charge (denoted SoC) C_{bat}: capacity of battery yields the quantity of energy
	expression between I_{10} and C_{10} current	$\frac{C_{bat}}{C_{10}} = \frac{1.65}{1+0.65.\left(\frac{I_{bat}}{I_{10}}\right)^{0.9}}(1+0.005.\Delta T)$	

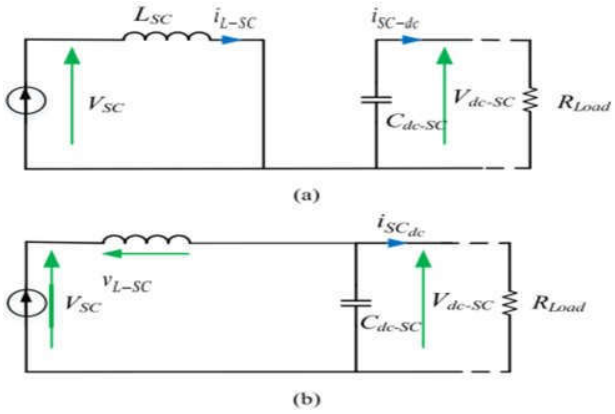

FIGURE 5.Electrical scheme of a buck-boost converter. a)Active phase b)Freewheeling phase

The main equation of the buck-boost converter is given by

$$L_{sc}\frac{d_{iL-sc}}{dt} = v_{sc} - (1 - d_{sc})v_{dc} \quad \text{……..(5)}$$

IV. CONTROL OF THE DC BUS VOLTAGE OF DIFFERENT SYSTEMS OF TRAIN AND STATION

Fig. 6 illustrates the basic operation of the SC, train, and stationary systems control systems. The reference current of the DC bus of the SC system, the train system, and the stationary system, $\mathrm{i}_{sc-dc-\mathrm{ref}}$, $\mathrm{i}_{bat-dcT-\mathrm{ref}}$, and $\mathrm{i}_{bat-dcS-\mathrm{ref}}$, are calculated by the PI controllers F(s), H(s), and J(s), respectively. The duty cycles of the stationary system D_S, train system D_T, and SC system D_{SC} are calculated by the PI controllers G(s), I(s), and K(s), respectively. A voltage control ensures. The management of the three DC buses. The following equations can be used to calculate the parameter of this PI controller (F(s), H(s) and J(s).

$$C_{dc-sc}\frac{dV_{dc-sc}}{dt} = \mathrm{i}_L - sc(1 - D_{sc}) - \frac{V_{dc-sc}}{r_{L-sc}} - \mathrm{i}_{sc-dc} \quad \text{…..……..(6)}$$

$$L_{sc}\frac{d_{iL-sc}}{dt} = v_{sc} - (1 - D_{sc})V_{dc} - sc \quad \text{...(7)}$$

Where $\beta_{sc} = 1 - D_{sc}$. Then,

$$C_{dc} - sc\frac{dV_{dc-sc}}{dt} = \mathrm{i}_L - sc\beta_{sc} - \frac{V_{dc-sc}}{r_{L-sc}} - \mathrm{i}_{sc-dc} \quad \text{……..……..(8)}$$

$$L_{sc}\frac{d_{iL-sc}}{dt} = V_{sc} - \beta_{sc}V_{dc} - sc \quad \text{……(9)}$$

Thereby, the dynamic equation is expressed as:

$$C_{dc-sc}\frac{dV_{dc-sc}}{dt} = \mathrm{i}_{\underset{V_{dc-sc}}{L}} - sc\frac{V_{sc}}{} - \frac{V_{dc-sc}}{r_{L-sc}} - \mathrm{i}_{sc-dc} \quad \text{……..(10)}$$

If X=$V_{dc}{}^2 - sc$ is changed, the linear function can be written as follows:

$$\frac{dX}{dt} = V_{dc} - sc\frac{dV_{dc-sc}}{dt} \quad \text{…….(11)}$$

Where

$$\frac{dV_{dc-sc}}{dt} = \frac{1}{2V_{dc-sc}}\frac{dX}{dt} \quad \text{……(12)}$$

$$C_{dc-sc}\frac{dX}{dt} = 2\mathrm{i}_L - scV_{sc} - 2\frac{X}{r_{L-SC}} - 2\mathrm{i}_{sc-dc}V_{dc} - sc \quad \text{…..……(13)}$$

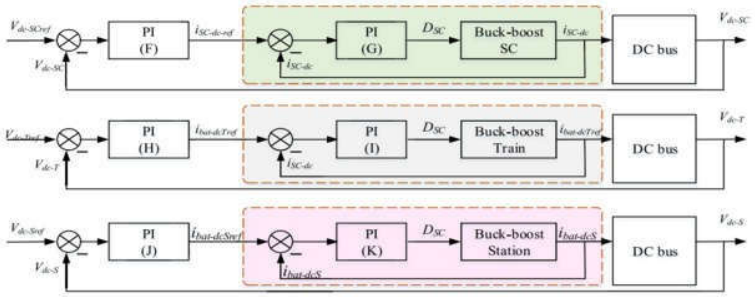

FIGURE 6. Block diagram of the energy management.

In the Laplace domain, the TF (transfer function) between voltage and current is given by

$$FT_{S(s)} == \frac{V_{dc-sc(s)}}{I_{sc-dc(s)}} = \frac{V_{sc}r_{L-sc}}{\frac{r_{L-sc}C_{dc-sc}}{2}s+1} \quad ...(14)$$

The TF of the SC system is represented by

$$F_{(S)} = K_{p-sc1} + \frac{K_{i-sc1}}{s} \quad .....(15)$$

where K_{i-sc1} and K_{p-sc1} are, respectively the integral gain and the proportional gain utilized for sc_s system control.

The train system's TF is depicted by

$$H_{(s)} = K_{p-T1} + \frac{K_{i-T_1}}{s} \quad ..(16)$$

The integral and proportional employed for train system control are respectively K_{i-T1} and K_{p-T1}. The following equation represents the stationary system's transfer function:

$$J_{(S)} = K_{p-s1} + \frac{K_{i-S_1}}{s} \quad .....(17)$$

The proportional and integral gains utilized for stationary system control are K_{i-s1} and K_{p-s1}, respectively. From equation (14) and (15) we deduce the following expression:

$$FTBF_{(s)} = \frac{K_{p-sc1}r_{L-sc}V_{sc}(s+\frac{k_{i-sc1}}{k_{p-sc1}})}{K_{p-sc1}r_{L-sc}V_{sc}(s+\frac{k_{i-sc1}}{k_{p-sc1}})+s(\frac{r_{L-sc}C_{dc-sc}}{2}s+1)} \quad (18)$$

$$FTBF_{(s)} = \frac{K_{p-sc1}r_{L-sc}V_{sc}(s+\frac{k_{i-sc1}}{k_{p-sc1}})}{\frac{r_{L-sc}C_{d-sc}}{2}s^2+(k_{p-sc1}r_{L-sc}V_{sc}+1)s+k_{p-sc1}r_{L-sc}V_{sc}\frac{k_{i-sc1}}{k_{p-sc1}}} \quad .....(19)$$

$$CLTF_{(S)} = \frac{\frac{2}{C_{dc-sc}}k_{p-sc}V_{sc}(s+\frac{k_{i-sc1}}{k_{p-sc1}})}{s^2+\frac{2}{r_{L-sc}C_{dc-sc}}(k_{p-sc1}r_{L-sc}V_{sc}+1)s+\frac{2}{C_{dc-sc}}V_{sc}k_{i-sc1}} \quad .....(20)$$

By comparing the denominator to that of the SC system's canonical form, we determine

$$\begin{cases} \omega_n^2 = \frac{2}{C_{sc}}VscK_{isc1} \quad .....(21) \\ k_{i-sc1} = \frac{\omega_{n-sc}{}^2C_{dc-sc}}{2V_{sc}} \end{cases}$$

$$\text{Where} \begin{cases} 2£_{SC}\omega_{n-sc} = \frac{2}{r_{L-SC}C_{dc-sc}}(k_{p-sc1}r_{L-sc}V_{sc}+1 \\ k_{p-sc1} = \frac{£_{SC}\omega_{n-sc}r_{L-SC}C_{dc-sc}-1}{r_{L-sc}V_{sc}} \end{cases} \quad ..(22)$$

Where ω_{n-sc} is the SC system's pulsation and $£_{SC}$ is its damping coefficient.

The integral and proportional employed for train system control are respectively K_{i-T1} and K_{p-T1}. They are communicated by:

$$K_{i-T1} = \frac{\omega_{n-T1}{}^2C_{dc-T}}{2V_{dc-T}} \quad .....(23)$$

$$K_{p-T1} = \frac{£T\omega_{n-T}r_{L-T}C_{dc-T}-1}{r_{L-T}V_{dc-T}} \quad ....(24)$$

When the train system's pulsation is represented by ω_{n-sc} and its damping coefficient is represented by $£_{SC}$.

The proportional and integral gains utilized for stationary system control are K_{i-S1} and K_{P-S1} respectively. They are communicated by:

$$K_{i-S1} = \frac{\omega_{n-S}{}^2-C_{dc-s}}{2V_{dc}} \quad .....(25)$$

$$K_{p-S1} = \frac{£_s \omega_{n-s} r_{L-S} C_{dc-s} - 1}{r_{L-s} 7_{dc}} \quad \text{……..…(26)}$$

When the stationary system's pulsation is represented by ω_{n-sc} and its damping coefficient is represented by $£_{SC}$.

A current control ensures the buck-boost converter's control. The following equations are used to calculate the parameters of this PI controller (G(s), I(s), and K(s)) according to the same methodology:

$$v_{sc} = L_{sc} \mathrm{i}_{L-SC}(s)s + R_{Load} \mathrm{i}_{L-SC}(s) + (1 - D_{sc}(s))V_{dc-sc} \quad \text{.....(27)}$$

The D_{sc} and I_{sc} is expressed as follows:

$$\frac{I_{sc}(s)}{D_{sc}(s)} = \frac{\frac{7_{dc-sc}}{RLoad}}{1+\frac{Lsc}{R_{Load}}s} \quad \text{……..(28)}$$

The TF of the SC system is given by the following equation.

$$\text{G(s)} = \frac{K_{\mathrm{i}-sc2}(1+\frac{\mathrm{k}p-sc2}{\mathrm{k}_{\mathrm{i}-sc2}}S)}{s} \quad \text{.....(29)}$$

The following equation translates the TF of the stationary system.

$$\text{I(s)} = \frac{K_{\mathrm{i}-T2}(1+\frac{K_{\mathrm{i}-T2}}{K_{\mathrm{i}-T2}}S}{s} \quad \text{……..(30)}$$

The following equation represents the stationary system's TF.

$$K(s) = \frac{K_{\mathrm{i}-S2}(1+\frac{K_{p-S2}}{K_{\mathrm{i}-S2}}S)}{S} \quad \text{……..(31)}$$

A pole/zero and imposing compensation are assumed to simplify the transfer function of the system: $\frac{\mathrm{k}_{p-SC2}}{\mathrm{k}_{\mathrm{i}-SC2}} = \frac{Lsc}{R_{load}}$. The new CLTF(s) becomes

$$\text{CLTF(s)} = \frac{1}{1+\frac{R_{Load}}{7_{dc-SC}K_{\mathrm{i}-SC2}}S} \quad \text{…….(32)}$$

Where

$$r_{SC} = \frac{R_{Load}}{V_{dc-SC}K_{\mathrm{i}-SC2}} \text{…….(33)}$$

Then, the integral and proportional employed for the SC system control are, respectively, $K_{\mathrm{i}-Sc2}$ and K_{p-Sc2}. They are communicated by:

$$K_{\mathrm{i}-SC2} = \frac{R_{Load}}{c_{SC}V_{dc-SC}} \quad \text{……(34)}$$

$$K_{p-SC2} = \frac{L_{SC}}{c_{SC}V_{dc-SC}} \quad \text{…….(35)}$$

$K_{\mathrm{i}-T2}$ and K_{P-T2} used for the train system control is expressed by:

$$K_{\mathrm{i}-T2} = \frac{R_{Load-SC}}{c_T V_{dc-T}} \quad \text{……(36)}$$

$$K_{p-T2} = \frac{L_{bat-T}}{c_T V_{dc-T}} \quad \text{…….(37)}$$

The integral and proportional used for train system control are $K_{\mathrm{i}-S2}$ and K_{P-S2} respectively. They are communicated by:

$$K_{\mathrm{i}-S2} = \frac{R_{Load-bat}}{c_S V_{dc-S}} \quad \text{…….(38)}$$

$K_{p-S2} = \frac{L_{bat-S}}{c_S V_{dc-S}}$ .....(39)

The time constants for stationary systems, trains, and SCs are, respectively, r_{SC}, r_S and r_T

V. SIMULATION RESULTS

The software MATLAB/Simulink creates a model of the entire system to examine the viability of the proposed plan. Two trains and one station (station 1) comprise the planned simulation test (train 1 and train2). The simulation experiments are suggested using the same train and station characteristics over a million years. Variable wind, sun radiation, and temperature scenarios are put out.

The station 1 batteries' starting state of charge is $SOC_{bat-Station1}$ = 30%.

The sc_s used in train 1 are initially charged to a state of charge $SoC_{sc-Train1}$ of 66%.

sc_s used in train 2 were initially charged to a state of charge $SoC_{sc-Train2}$ of 66%.

The simulation test of station 1 is shown in Fig. 7. A microgrid using PV and wind as sources has suggested this station. Batteries provide insurance for the energy storage. The simulation tests for trains 1 and 2 are shown in Figs. 8 and 9, respectively. Trains 1 and 2 charge from

station 1 at different times during this simulation test. Train 1 arrives at Station 1 in 50 seconds while Train 2 arrives in 650 seconds. The PV and wind are shown in Fig. 7(a). that is varied between 1200A and 3000A.Fig. 7 depicts the charge current of station 1 (b).

Train 1 is charged from station 1 for a time of between t=50 and t=350 seconds at a constant current of IchargeStation1 = 1000A.five minutes long. Train 2 charges from station 1 for five minutes with a steady current of IchargeStation1 = 1000A between t=650 and t=950. Fig. 7 displays the station 1 DC bus voltage (c). 500V is the set value. Fig. 7 displays the batteries' current state of charge for station 1. (d).It is between 30% and 50% represented. Train 1 charges between t=50 and t=350 from station 1, and between t=800 and t=1000 from station 2. Fig. 8(a and b) shows the charge current of the sc_s from stations 1 and 2 that were used for train 1. Figure 8(c and d) displays the power and current of sc_s, respectively. In the charging mode, power and current are constant and positive, but they are variable and negative in the traction mode. As seen in Fig. 8, train 1's DC bus voltage is 2000V. (e).Fig. 8 displays the stat of charge for the sc_s of train 1. (f). It ranges between 61% and 67% and shows an increase when the vehicle is charging and a decrease when it is in traction mode. Between t=650s and t=950s, Train 2 accelerates out of Station 1.

It fluctuates between 69% and 66%, indicating an increase during charging mode and a decrease during traction mode.

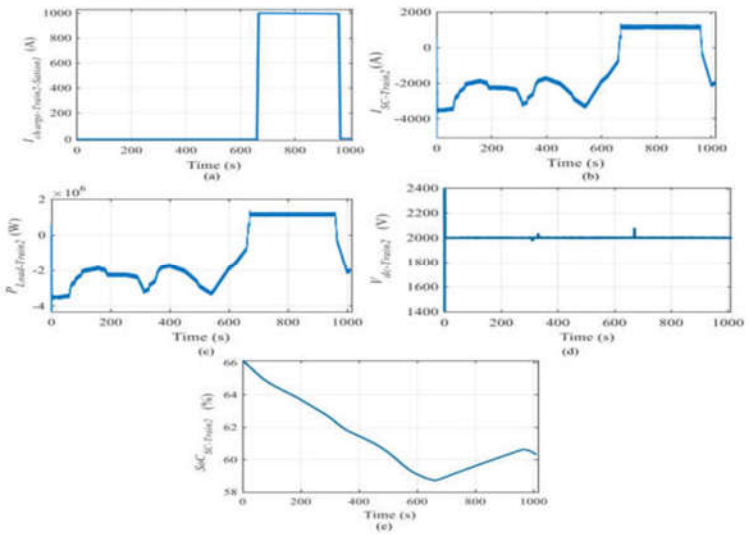

FIGURE 9. Simulation test of train 2. (a) Charge current of train 1 from station 1. (b) SCs current of train 2. (c) Load power of train 2. (d) DC bus voltage of train 2. (e) SoC of SCs of train 2.

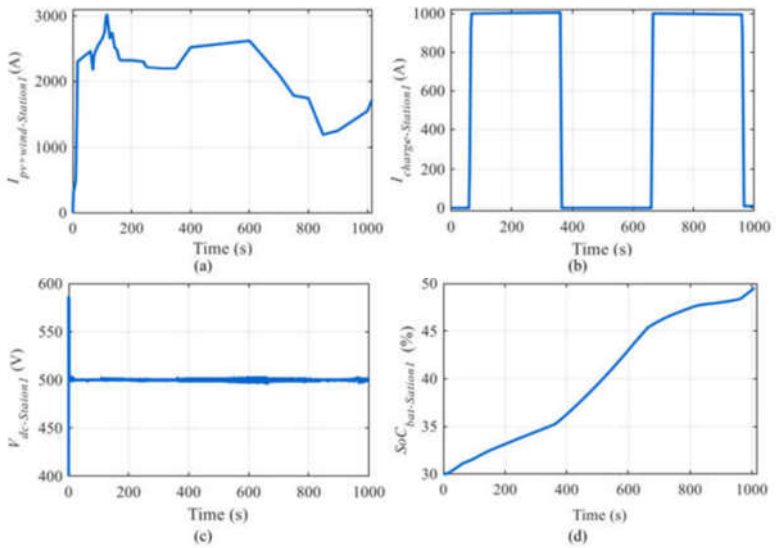

FIGURE 7. Simulation test of station 1. (a) PV and wind current of station 1. (b) Charge current from station 1. (c) DC bus voltage of station 1. (d) SoC of batteries of station 1

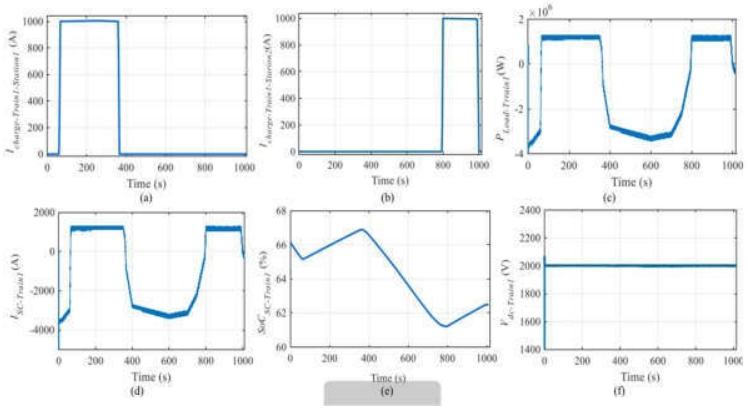

FIGURE 8. Simulation test of train 1. (a) Charge current of train 1 from station 1. (b) Charge current of train 1 from station 2. (c) Load power of train 1. (d) SCs current of train 1. (e) SoC of SCs of train 1. (f) DC bus voltage of train 1.

VI. CONCLUSION:

This research provided the proposed techno-economic method for the energy storage utilizing sc_s in the train. The station and train are the two components of the analyzed system. Utilizing PV and wind as the primary energy sources, along with batteries for ESS, the architecture of a railroad station is illustrated. The engine and sc_s make up the train. A pantograph mounted on an air power line at each stop supplies sc_s to the train's ESS, where they are fed from the stations and breaking phases. sc_s are used because they charge and discharge quickly. In order to stabilize the DC bus, an EMS is administered. The buck-boost converter's calculation of its parameters is given. The integral and proportional gain controller's size, which is utilized to stabilize the DC bus of trains and stations, is provided. an exam that simulates was suggested to have two trains and one station. The station is where the trains refuel at various intervals. The outcomes demonstrated that the proposed EMS and system design perform well in stabilizing the DC bus voltage and responding to the engine's demand for energy. The use of this technique with an AC engine will be the focus of future studies.

REFERENCES

[1] G. Cui, L. Luo, C. Liang, S. Hu, Y. Li, Y. Cao, B. Xie, J. Xu, Z. Zhang, Y. Liu, and T. Wang, ‘‘Supercapacitor integrated railway static power conditioner for regenerative braking energy recycling and power quality improvement of high-speed railway system,’’ IEEE Trans. Transport. Electrific., vol. 5, no. 3, pp. 702–714, Sep. 2019.

[2] F. Ciccarelli, A. Del Pizzo, and D. Iannuzzi, ‘‘Improvement of energy efficiency in light railway vehicles based on power management control of wayside lithium-ion capacitor storage,’’ IEEE Trans. Power Electron., vol. 29, no. 1, pp. 275–286, Jan. 2014.

[3] V. A. Kleftakis and N. D. Hatziargyriou, ‘‘Optimal control of reversible substations and wayside storage devices for voltage stabilization and energy savings in metro railway networks,’’ IEEE Trans. Transport. Electrific., vol. 5, no. 2, pp. 515–523, Jun. 2019.

[4] T. Ratniyomchai, S. Hillmansen, and P. Tricoli, ‘‘Recent developments and applications of energy storage devices in electrified railways,’’ IET Elect. Syst. Transp., vol. 4, no. 1, pp. 9–20, Mar. 2014.

[5] H. Yang, W. Shen, Q. Yu, J. Liu, Y. Jiang, E. Ackom, and Z. Y. Dong, ‘‘Coordinated demand response of rail transit load and energy storage system considering driving comfort,’’ CSEE J. Power Energy Syst., vol. 6, no. 4, pp: 749-759, Dec. 2020.

[6] H. Yang, J. Zhang, J. Qiu, S. Zhang, M. Lai, and Z. Y. Dong, ‘‘A practical pricing approach to smart grid demand response based on load classification,’’ IEEE Trans. Smart Grid, vol. 9, no. 1, pp. 179–190, Jan. 2018.

[7] Z. Cabrane, M. Ouassaid, and M. Maaroufi, ‘‘Analysis and evaluation of battery-supercapacitor hybrid energy storage system for photovoltaic installation,’’ Int. J. Hydrogen Energy, vol. 41, no. 45, pp. 20897–20907, Dec. 2016.

[8] Z. Cabrane, J. Kim, K. Yoo, and M. Ouassaid, ‘‘HESS-based photovoltaic/batteries/supercapacitors: Energy management strategy and DC bus voltage stabilization,’’ Sol. Energy, vol. 216, pp. 551–563, Mar. 2021.

[9] Q. Z. Li, X. J. Wang, X. H. Huang, Y. Zhao, Y. W. Liu, and S. F. Zhao, ‘‘Research on flywheel energy storage technology for electrified railway,’’ Proc. CSEE, vol. 39, no. 7, pp. 2025–2033, Apr. 2019.

[10] H. Yang, Q. Yu, J. Liu, Y. Jia, G. Yang, E. Ackom, and Z. Y. Dong, ‘‘Optimal wind-solar capacity allocation with coordination of dynamic regulation of hydropower and energy intensive controllable load,’’ IEEE Access, vol. 8, pp. 110129–110139, 2020.

[11] M. Andriollo, R. Benato, M. Bressan, S. Sessa, F. Palone, and R. Polito, ‘‘Review of power conversion and conditioning systems for stationary electrochemical storage,’’ Energies, vol. 8, no. 2, pp. 960–975, Jan. 2015, doi: 10.3390/en8020960.

[12] K. C. Divya and J. Østergaard, ‘‘Battery energy storage technology for power systems—An overview,’’ Electr. Power Syst. Res., vol. 79, no. 4, pp. 511–520, Apr. 2009.

[13] I. Hadjipaschalis, A. Poullikkas, and V. Efthimiou, ‘‘Overview of current and future energy storage technologies for electric power applications,’’ Renew. Sustain. Energy Rev., vol. 13, nos. 6–7, pp. 1513–1522, 2009.

[14] Z. Cabrane and S. H. Lee, ‘‘Electrical and mathematical modeling of supercapacitors: Comparison,’’ Energies, vol. 15, no. 3, p. 693, Jan. 2022.

[15] Z. Cabrane, M. Ouassaid, and M. Maaroufi, ‘‘Battery and supercapacitor for photovoltaic energy storage: A fuzzy logic management,’’ IET Renew. Power Gener., vol. 11, no. 8, pp. 1157–1165, 2017. [16] Z. Yang, F. Zhu, and F. Lin, ‘‘Deep-reinforcement-learning-based energy management strategy for supercapacitor energy storage systems in urban rail transit,’’ IEEE Trans. Intell. Transp. Syst., vol. 22, no. 2, pp. 1150–1160, Feb. 2021.

[17] D. Roch-Dupré, T. Gonsalves, A. P. Cucala, R. R. Pecharromán, Á. J. López-López, and A. Fernández-Cardador, ‘‘Multi-stage optimization of the installation of energy storage systems in railway electrical infrastructures with nature-inspired optimization algorithms,’’ Eng. Appl. Artif. Intell., vol. 104, Sep. 2021, Art. no. 104370.

[18] H. Lee, S. Jung, Y. Cho, D. Yoon, and G. Jang, ‘‘Peak power reduction and energy efficiency improvement with the superconducting flywheel energy storage in electric railway system,’’ Phys. C, Supercond. Appl., vol. 494, pp. 246–249, Nov. 2013.

[19] S. Khayyam, N. Berr, L. Razik, M. Fleck, F. Ponci, and A. Monti, ‘‘Railway system energy management optimization demonstrated at offline and online case studies,’’ IEEE Trans. Intell. Transp. Syst., vol. 19, no. 11, pp. 3570–3583, Nov. 2018.

[20] Z. Cabrane, J. Kim, K. Yoo, and S. H. Lee, ‘‘Fuzzy logic supervisor based novel energy management strategy reflecting different virtual power plants,’’ Electr. Power Syst. Res., vol. 205, Apr. 2022, Art. no. 107731.

[21] H. Peng, J. Li, L. Lowenstein, and K. Hameyer, ‘‘strategy based on optimal control theory for a fuel cell hybrid railway vehicle,’’ Appl. Energy, vol. 267, Jun. 2020, Art. no. 114987.

[22] X. Jiang and S. Wang, ‘‘Railway panorama: A fast inspection method for high-speed railway infrastructure monitoring,’’ IEEE Access, vol. 9, pp. 150889–150902, 2021.

[23] C. Feng, Z. Gao, Y. Sun, and P. Chen, ‘‘Electric railway smart microgrid system with integration of multiple energy systems and powerquality improvement,’’ Electr. Power Syst. Res., vol. 199, Oct. 2021, Art. no. 107459.

[24] Q. Zhang, Z. Yuan, L. Yan, T. Zhang, Y. Miao, and S. Ding, ‘‘A railway train number tracking method using a prediction approach,’’ IEEE Access, vol. 7, pp. 138288–138298, 2019.

[25] W. He, W. Shi, J. Le, H. Li, and R. Ma, ‘‘Geophone-based energy harvesting approach for railway wagon monitoring sensor with high reliability and simple structure,’’ IEEE Access, vol. 8, pp. 35882–35891, 2020.

[26] Y. Sun, Y. Cao, M. Zhou, T. Wen, P. Li, and C. Roberts, ‘‘A hybrid method for life prediction of railway relays based on multi-layer decomposition and RBFNN,’’ IEEE Access, vol. 7, pp. 44761–44770, 2019.

[27] H. Novak, V. Lešić, and M. Vašak, ‘‘Hierarchical model predictive control for coordinated electric railway traction system energy management,’’ IEEE Trans. Intell. Transp. Syst., vol. 20, no. 7, pp. 2715–2727, Jul. 2019.

[28] G. Graber, V. Calderaro, V. Galdi, A. Piccolo, R. Lamedica, and A. Ruvio, ‘‘Techno-economic sizing of auxiliary-battery-based substations in DC railway systems,’’ IEEE Trans. Transport. Electrific., vol. 4, no. 2, pp. 616–625, Jun. 2018.

[29] D. Rekioua, S. Bensmail, and N. Bettar, ‘‘Development of hybrid photovoltaic-fuel cell system for stand-alone application,’’ Int. J. Hydrogen, vol. 39, pp. 1604–1611, Jan. 2014.

[30] A. Lahyani, P. Venet, A. Guermazi, and A. Troudi, ‘‘Battery/supercapacitors combination in uninterruptible power supply (UPS),’’ IEEE Trans. Power Electron., vol. 28, no. 4, pp. 1509–1522, Apr. 2013.